Zoological Journal of the Linnean Society, 2023, **199**, 994–1012
https://doi.org/10.1093/zoolinnean/zlad074
Advance access publication 9 August 2023
Original Article

OXFORD

Original Article

Ecomorphological correlates of inner ear shape in Australian limb-reduced skinks (Scincidae: Sphenomorphini)

Marco Camaiti[1,*], James Wiles[1], Rocio Aguilar[2], Mark N. Hutchinson[3–5], Christy A. Hipsley[2,6,7], David G. Chapple[1,‡], Alistair R. Evans[1,‡]

[1]School of Biological Sciences, Monash University, Clayton, Victoria, Australia
[2]Department of Sciences, Museums Victoria, Carlton, Victoria, Australia
[3]South Australian Museum, Adelaide, South Australia, Australia
[4]School of Biological Sciences, University of Adelaide, Adelaide, South Australia, Australia
[5]Faculty of Science and Engineering, Flinders University of South Australia, Bedford Park, South Australia, Australia
[6]School of Biosciences, University of Melbourne, Parkville, Victoria, Australia
[7]Department of Biology, University of Copenhagen, Copenhagen, Denmark

‡Joint senior authors.

[*]Corresponding author. School of Biological Sciences, Monash University, Clayton, Victoria, Australia. tel. +61481981104. E-mail: marco.camaiti@monash.edu

ABSTRACT

The inner ear labyrinth is an organ able to perceive balance and spatial orientation, but the drivers of its morphological variation across and within vertebrate lineages are unclear. We assess two competing hypotheses whether this organ, and specifically the semicircular canals, modifies its shape as a functional adaptation to ecology and locomotion, or according to the constraints of skull morphology. We test these using 52 species of Australian sphenomorphines, a group of scincid lizards that evolved changes in body shape and locomotory adaptations to fossoriality multiple times independently, by reducing their limbs. We find a correlation between semicircular canal shape and degree of limb reduction in these lizards, supporting a functional hypothesis. The interaction between body shape and substrate ecology is also a significant predictor. The wider and more eccentric semicircular canals of limb-reduced skinks indicate higher balance sensitivity and manoeuvrability compared with fully limbed skinks, probably as an adaptation to navigating cluttered environments. Conversely, our results show only a minimal influence of skull constraints on semicircular canal shape, having instead significant effects on size. This supports the hypothesis that in these skinks inner ear shape evolution is driven by specific locomotory strategies more than it is constrained by cranial anatomy.

Keywords: inner ear; ecomorphologylimb reduction; skinks; bony labyrinth

INTRODUCTION

The inner ear labyrinth is an important sensory organ in vertebrates, able to capture sound, gravity, and head movements (Steinhausen 1933, Wever 1978, Wilson and Melvill Jones 1979, Oman *et al.* 1987, Rabbitt *et al.* 2004). This organ, housed in a pair of mirrored cavities in the posterolateral sides of the neurocranium, has its most prominent feature in the vestibular system, composed of the three semicircular canals, which surround a central, rounded structure known as the saccule or vestibule (Evans 2016) (Fig. 1A, B). Within the bone cavity of the labyrinth are encased ducts lined with soft ciliated tissue and filled with liquid. When the head is rotated or movement is detected, shifts in the liquid stimulate the ciliated tissue to send signals to the brain (Muller 1994). Semicircular canals perceive rotational changes and angular accelerations, whereas the saccule's main function is to detect linear accelerations of gravitational and inertial origin (Rabbitt *et al.* 2004, Goyens and Aerts 2018). Together, these constitute the main balance organ in vertebrates (Oman *et al.* 1987).

Labyrinth shape has been hypothesized to be a predictor of the patterns of locomotion of various lineages of vertebrate taxa. Shape variations in eccentricity, relative length, and/or orthogonality between canals can have measurable effects in terms of vestibular system sensitivity to head movements (Cox and Jeffery 2010 Benson *et al.* 2017, Gonzales *et al.* 2019), which can be linked with agility, thus embodying the complexity of the

Received 8 February 2023; revised 14 May 2023; accepted 24 May 2023

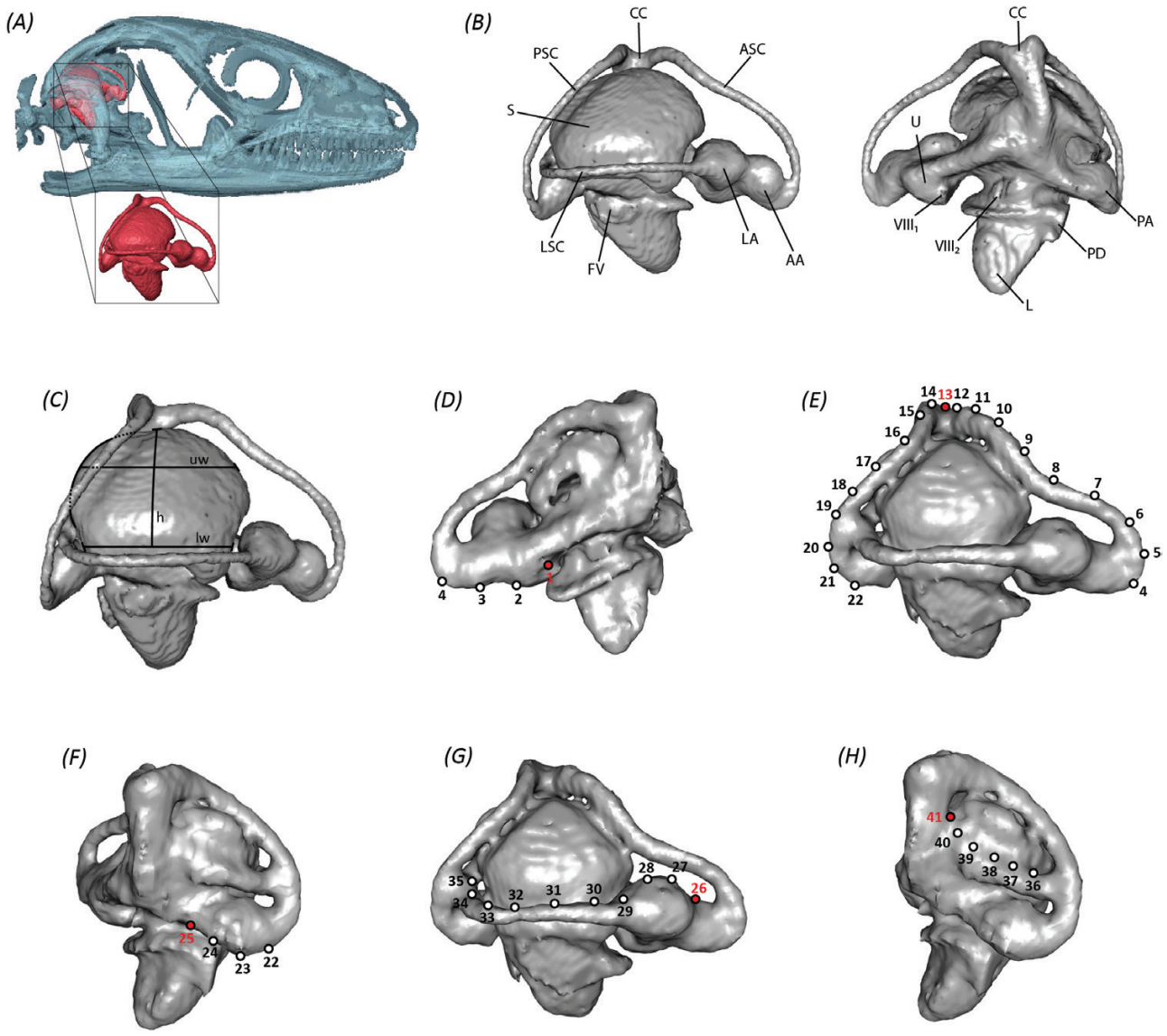

Figure 1. Digital endocasts of the labyrinth of *Ctenotus robustus* (MV-D52574: A, B, C) and *Hemiergis millewae* (MV-D63760: D-H). A, positioning in the skull of the inner ear labyrinth. B, anatomical atlas of the inner ear labyrinth, seen from the lateral and medial side, after the terminology by Palci *et al.* (2017). Abbreviations: VIII1, anterior branch of the auditory nerve (partial); VIII2, posterior branch of the auditory nerve (partial); AA, anterior ampulla; ASC, anterior semicircular canal; CC, crus commune; FV, fenestra vestibuli; L, lagena; LA, lateral ampulla; LSC, lateral semicircular canal; PA, posterior ampulla; PD, perilymphatic duct (partial); PSC, posterior semicircular canal; S, saccule (vestibule); U, utricle. C, measurements taken for saccular (vestibular) proportions. Abbreviations: h, saccular height; uw, saccular width at the top; lw, saccular width at the bottom. D–H, protocol used for landmarking the specimens in our dataset. Red dots indicate fixed landmarks, white dots indicate sliding semilandmarks.

range of movement allowed by an animal's locomotory pattern (Vasilopoulou-Kampitsi *et al.* 2019b). Semicircular canal sensitivity can be split into two main components: the response time to rotational accelerations, and signal discrimination (Rabbitt *et al.* 2004). Response time to rotational accelerations has been linked to the cross-section of semicircular canal ducts, as it alters the flow speed of the endolymphatic liquid that transmits the signal: the smaller the cross-sectional area of the canals, the higher the speed of the fluid and the subsequent signal transmission (Rabbitt *et al.* 2004, Spoor *et al.* 2007). Signal discrimination, or the threshold of detection of accelerations in head rotation (Rabbitt *et al.* 2004), has been found to associate with semicircular canals with higher orthogonality between them (Malinzak *et al.* 2012), and larger and more circular radii of the semicircular canal arcs (Spoor and Zonneveld 1995, Yang and Hullar 2007, Ekdale 2016), especially the lateral one (Cox and Jeffery 2010). This latter aspect is thought to permit higher manoeuvrability during locomotion (Cox and Jeffery 2010 Vasilopoulou-Kampitsi *et al.* 2019b).

Indeed, functional studies have linked inner ear shape variations with differential locomotory capabilities that relate to different patterns of habitat use (Dickson *et al.* 2017, Capshaw *et al.* 2019), and with predator avoidance in simple, open environments (Vasilopoulou-Kampitsi *et al.* 2019b), tying labyrinth shape to particular ecomorphologies. The functional and ecological signal of semicircular canal shape has also been

thoroughly explored in fields such as palaeontology, in which inner ear endocasts are used to predict the locomotion patterns and ecology of extinct species by comparing them with extant ones (e.g. anoles: Dickson *et al.* 2017; non-avian dinosaurs: Hanson *et al.* 2021, David *et al.* 2022). These functional assessments have been largely focused on the meaning of variations in semicircular canal shape and not diameter (with some exceptions, i.e. Hanson *et al.* 2021), finding that signal discrimination is the main aspect that correlates with locomotion and agility, instead of response time. In our paper, which is also focused on the functionality of semicircular canal morphologies, we will be considering exclusively this aspect when discussing sensitivity. Beyond the shape of the semicircular canals, the proportions of the saccule relative to the semicircular canals have been shown to vary dramatically across ecomorphs, showing that inflated saccules are prominently present in some burrowing animals (i.e. snakes: Yi and Norell 2015, Capshaw *et al.* 2019, Yi 2022). In general, these considerations of both shape and size can be seen as extensions of the functional hypothesis, as different ecomorphs would correspond to different functional (and thus often locomotory in nature) interactions within a given environmental niche.

What remains unclear is how, and why, variations in locomotory capabilities translate into shape changes that might in turn induce alterations in the functionality (i.e. sensitivity, speed of sensory impulse) of the inner ear (Evers *et al.* 2022). Some authors (Ramprashad *et al.* 1986, Benson *et al.* 2017, Costeur *et al.* 2018, Bronzati *et al.* 2021, David *et al.* 2022, Evers *et al.* 2022) have pointed out how variations in semicircular canal shape might not correspond to differential sensory capabilities, indicating that very different semicircular canal shapes can have similar outcomes in terms of sensitivity and functional performance, and casting doubt on the functionality argument. Specifically, studies such as Bronzati *et al.* (2021) on archosaurs and Evers *et al.* (2022) on turtles found locomotory and ecomorphological factors to have lower explanatory power than allometry or spatial constraints of the braincase when tested together in predictive models of inner ear shape, questioning the validity of semicircular canal shape as a consistent predictor of ecomorphological associations and locomotion in extant and fossil taxa. Studies such as Palci *et al.* (2017) on snakes, Evers *et al.* (2022) on turtles, and Costeur *et al.* (2018) on toothed whales have questioned the validity of semicircular canal shape as a consistent predictor of ecomorphological associations in extant and fossil taxa. On the other hand, studies such as Benson *et al.* (2017) on birds, Costeur *et al.* (2018) on toothed whales, and David *et al.* (2022) on non-avian dinosaurs indicate that other factors, such as relative labyrinth size and cochlear shape, may, from a biomechanical standpoint, be more important in determining ecological and locomotory differences in canal function than semicircular canal shape variation.

Additionally, accounting for phylogenetic relatedness when exploring ecological signal often reveals weak, or non-existent, associations between semicircular canal shape and ecology and locomotory modes compared to naïve analyses, showing them to be at best secondary compared with phylogenetic signal or allometry (Dickson *et al.* 2017, Palci *et al.* 2017, Evers *et al.* 2022). This has introduced the hypothesis—contrasting with the functional/ecological signal hypothesis—that part of the variation seen in vertebrate inner ears may be subject to the spatial constraints of the skull (Rieppel 1984, Evers *et al.* 2022). During development, both the size and shape of the vestibular system would be limited in how much space they can occupy in the neurocranium, which would, for example, explain variations in semicircular canal eccentricity (Goyens 2019). These constraints have been shown to constitute a trade-off with the sensitivity of these organs, as sensitivity significantly decreases with eccentricity of semicircular canals (Goyens 2019). This highlights the need for more insight in exploring these relationships, including the consideration of understudied groups, across a wider variety of evolutionary lineages, ecologies, and functional interactions with the environment. As recent studies (i.e. Evers *et al.* 2022) have demonstrated, testing the relative strength of ecological variables and ontogenetic constraints in a phylogenetic framework represents the optimal way forward in addressing the probable causes of variation in inner ear shape.

Reptiles, and especially lizards and snakes (Squamata), provide excellent model systems to examine questions regarding semicircular canal shape and its relationship with ecology, as they tend to be highly diversified in terms of their ecologies and locomotory modes, which often correspond to different external morphologies (Garland and Losos 1994). In these regards, the squamate clades that have received most attention are snakes (Yi and Norell 2015, Palci *et al.* 2017), anoles (Dickson *et al.* 2017), and lacertid lizards (Vasiloupolou-Kampitsi *et al.* 2019a, b). Skinks (Squamata: Scincidae) are an interesting lineage because, in addition to being species-rich (1743 species are currently listed in the Reptile Database: Uetz *et al.* 2022), globally widespread, and inhabiting a wide variety of environments, they also display a striking array of morphologies that reflect their adaptations to their environments. One such, and perhaps most dramatic, morphological transformation is limb reduction, which has happened more often in skinks than in any other squamate (or tetrapod) group, having evolved an estimated 53 to 71 times independently across lineages and geographical regions (Camaiti *et al.* 2022). Limb reduction tends to be associated with the miniaturization and loss of elements of the limbs (including digits and limb bones), and relative elongation of the trunk by the addition or elongation of presacral vertebrae (Camaiti *et al.* 2021), and miniaturization of the skull to match the reduced cross-sectional area of the body (Rieppel 1984). These morphological changes were found to be linked with shifts from a limb-powered locomotion to an axial-powered, undulatory locomotion, which generally correspond to adaptations to living inside or in close contact with complex three-dimensional environments like the substrate, which in fact classifies most of these lizards as fossorial or substrate-swimming. As limb-reduced lizards have often greatly modified the shapes of their skulls for better penetration in the substrate (Vanhooydonck *et al.* 2011, Le Guilloux *et al.* 2020; Stepanova and Bauer 2021), we expect that semicircular canal shape in these taxa would change to adapt to different balance and sensitivity conditions presented by subterranean environments. In skinks, the existing range of limb-reduced morphs can be associated with different substrate ecologies and degrees of fossoriality (Wiens and Slingluff 2001, Camaiti *et al.* 2021, 2022, 2023), making them a model system to study and interpret this phenomenon at a fine scale. This makes it possible to directly test the ecomorphological correlates of labyrinth shape and size.

In this study, we use 3D geometric morphometrics to examine the ecological and morphological correlates of the inner ears of a sample of 52 Australian skink species belonging to the tribe Sphenomorphini, (subfamily Lygosominae: Shea 2021). This lineage is one of the most diverse among skinks for the number of independent times it evolved limb reduction [at least 22 times according to the estimate of Camaiti *et al.* (2022)], as well as conveniently including representatives of the full spectrum of limb reduction, from limbed to limbless, with intermediate forms in-between (Greer 1989, Camaiti *et al.* 2022). They are also one of the most ecologically diverse vertebrate groups of Australia (Greer 1989). Specifically, we aim to contrast and test two competing, non-mutually exclusive hypotheses to explain the variation in inner ear morphology: (i) that the shape of the vestibular system, specifically the semicircular canals, carries ecological signal and/or relates to locomotion; and (ii) that it is subject to other factors such as allometry and the developmental constraints of cranial architecture. We test the relationships between semicircular canal morphology, limb status (i.e. fully limbed, moderately or dramatically limb-reduced, limbless), and body proportions, to estimate the effect of varied locomotory strategies on the vestibular system. We also test the differential variation in these variables (as well as allometric relationships and skull dimensions) across ecomorphs and substrate ecomorph categories (Camaiti *et al.* 2022, 2023).

MATERIALS AND METHODS

Specimens, data acquisition, and landmark protocol

We acquired high-resolution X-ray computed tomographies (CT-scans) of 52 specimens of Australian skinks using a Skyscan 1076 scanner at Adelaide Microscopy (University of Adelaide, Adelaide, South Australia), and a Phoenix Nanotom micro-CT scanner at the University of Melbourne School of Geography, Earth and Atmospheric Sciences TrACEES Platform (University of Melbourne, Melbourne, Victoria). We used the software AVIZO (v.2022) to reconstruct and visualize 3D volumes from stacks of '.bmp' and '.tif' image files. Using the same software, we segmented (digitally isolated) the endocasts of the right inner ears of the specimens and then converted them to 3D '.ply' file meshes.

Landmarks and semilandmarks were placed on meshes using IDAV Landmark Editor (v.3.6), based on the procedure illustrated by Palci *et al.* (2017). Fixed landmarks were placed in the same points illustrated by Palci *et al.* (2017) and sliding semilandmarks were placed in the same order (Fig. 1D–G). Compared to Palci *et al.* (2017), sliding semilandmarks were placed in different densities along curves due to the different shape and relative lengths of the semicircular canals in our sample, probably linked to anatomical differences between snakes and skinks. The first fixed landmark was placed where the saccular cavity encounters the notch of the anterior branch of the VIII nerve (Fig. 1D). Eleven sliding semilandmarks (instead of 14), were then placed along the exterior curvature of the anterior semicircular canal, facing away from the saccule (Fig. 1D, E). The second fixed landmark (landmark 13), which represents both the endpoint of the anterior semicircular canal curve and the starting point of the posterior semicircular canal curve, was placed on the top of the crus commune (Fig. 1E). We placed 11 semilandmarks (instead of 13) on the line of maximum curvature of the posterior semicircular canal, on the side facing away from the saccule (Fig. 1E, F). At the end of this curve, we placed a fixed landmark (landmark 25), which is located at the approximate point of intersection between the ampulla and the saccule (Fig. 1F). Fixed landmark 26 was placed at the groove separating the anterior and the posterior ampullae, keeping the lateral semicircular canal horizontal (Fig. 1G). Dorsolaterally along the lateral semicircular canal, we placed 14 (instead of 13) sliding semilandmarks (Fig. 1G, H). The last landmark of the lateral semicircular canal curve (landmark 41) was fixed and placed at the posterior end of the lateral semicircular canal, where it converges near the crus commune (Fig. 1H). In contrast to Palci *et al.*, (2017), no landmarks were placed on the centre of the saccule, or at the crux between the anterior and posterior semicircular canal, or at the point of maximum curvature at the bottom of the lagena, as we were unable to place them consistently. The landmark configurations for all specimens are provided in Supporting Information, Material S1A.

All species and specimen numbers are available in Supporting Information, Material S1B. Each specimen represents a distinct species of skink (Squamata: Scincidae), belonging to the Australian branch of the tribe Sphenomorphini (Fig. 2). Five focal clades are represented where limb reduction and fossorial adaptations evolved at least once: *Anomalopus*, *Glaphyromorphus*, *Hemiergis*, *Lerista*, and *Saiphos* (Fig. 3). The *Saiphos* clade includes more genera (*Coggeria*, *Coeranoscincus*, *Ophioscincus*, and *Saiphos*, as per Skinner *et al.* 2013). Where possible, we included at least a fully limbed species from a sister-taxon for each clade [except for *Anomalopus*, as the genus does not have any immediate fully limbed sister-taxa: see mapped phylogeny by Camaiti *et al.* (2022)]. To test for associations between inner ear morphology and general body shape, we also sourced morphometric measurements (head length, snout–vent length, limb lengths) for each species from Camaiti *et al.* (2022) and Camaiti *et al.* (2023). For species not included in those datasets (*Calyptotis lepidorostrum*, *Concinnia tenuis*, *Eulamprus kosciuskoi*, and *Glaphyromorphus cracens*), we sourced measurements directly from our specimen scans using the distance measuring tool in AVIZO (v.2022). For all species, we also calculated the limb disparity index based on the definition by Camaiti *et al.* (2023) using limb measurements. We assigned limb status (i.e. fully limbed, limb-reduced, or limbless) to each species based on the dataset by Camaiti *et al.* (2022) or, lacking that, based on the measurements taken directly from the scans. Based on the definition of Camaiti *et al.* (2022), to qualify as limb-reduced, a species must have forelimb lengths ≤ 15% and/or hindlimb lengths ≤ 20% of snout–vent length, while limbless species completely lack limbs. To better discriminate between different degrees of limb reduction, we further divided limb-reduced species between highly reduced, when having the length of at least one of the limb pairs ≤ 5% of SVL, and the rest as moderately reduced (Fig. 2).

For all specimens in our study, we used the AVIZO (v.2022) distance-measuring tool to obtain skull dimensions: length (distance from the tip of the premaxilla to the end of the occipital condyle), width (distance between

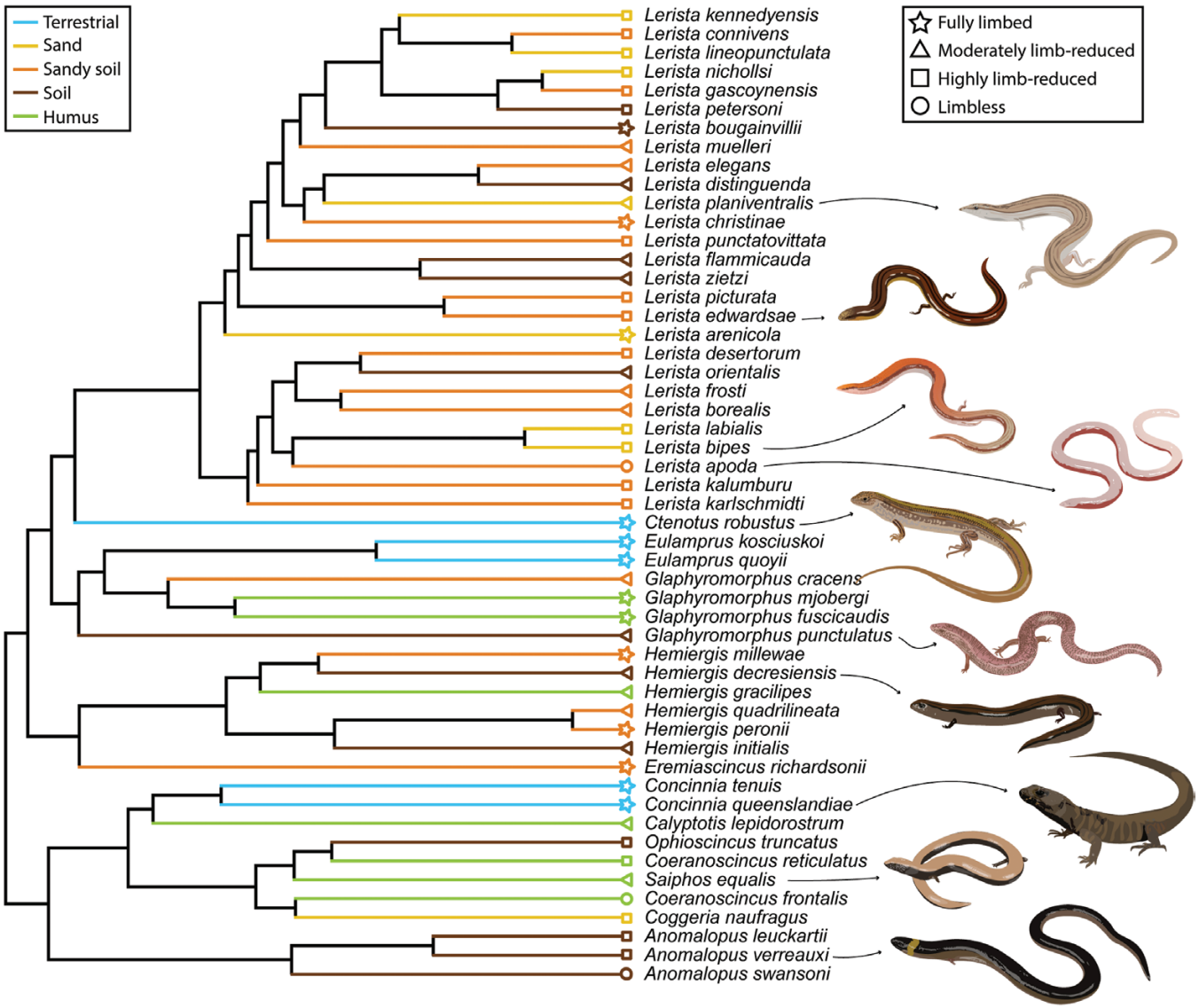

Figure 2. Phylogenetic tree of the taxa included in our analysis (pruned from the phylogeny of Zheng and Wiens 2016), coloured by categories of substrate ecology. Different symbols at the tips of the tree indicate different degrees of limb reduction. Illustrations represent the taxa indicated by the arrows (not to scale).

the two paraoccipital processes of the neurocranium), and height (distance between the anteriormost projection of the sphenoid and the posterior edge of the parietal foramen). The variable skull cuboid volume, indicating the volume of the solid defined by the maximum dimensions of the skull, was obtained by multiplying these three measures. To quantify the proportions of the saccule for each species, we used the same tool to measure three standardized saccular dimensions: height (from the highest point of the saccule at the crus commune to the border of the groove of the lateral semicircular canal, perpendicular with the plane passing through the lateral semicircular canal), width at the top (between the midpoint of the posterior bulge of the saccule and the anterior bulge, parallel with the plane passing through the lateral semicircular canal), width at the bottom (between the lowest point of the posterior edge of the posterior semicircular canal groove to the anterior edge of the saccule where it meets the lateral semicircular canal ampulla dorsally) (Fig. 1B).

To estimate the differentiation in ear shape depending on the ecomorph the species belong to, we categorized species based on the categories of substrate ecology of Camaiti *et al.* (2022, 2023; see Fig. 2). These include species living in humus, soil, sandy soil, and sand, as well as surface-dwelling, 'terrestrial' category species. This categorization, similar to the one of Stepanova and Bauer (2021), was justified by the findings of Camaiti *et al.* (2023), indicating that distinct substrate ecologies correspond to distinct body shapes and locomotory strategies. We also included a simplified ecomorphological characterization grouping all non-surface-dwelling species in the 'fossorial' category. As not all the species in our sample are present in that database, we scored three species for both characterizations based on field guides and the available literature for those species (Supporting Information, Material S2).

Data analysis

After exporting the landmark configurations, we scaled and aligned the specimens via Procrustes superimposition with the

'gpagen' function in the R package GEOMORPH (v.3.3.1), specifying which landmarks were fixed and which were semilandmarks. To validate our landmark placement procedure, we re-landmarked a random subset of our specimens five times, each using the same protocol, and included them in a PCA to visualize their differences (Supporting Information, Material S3).

We estimated phylogenetic signal K_{mult} of inner ear shape with the 'physignal' function in the package GEOMORPH (v.3.3.1: Adams *et al.* 2022). We further estimated univariate phylogenetic signal K for centroid size using the 'phylosig' function in the package PHYTOOLS (v.0.7.7: Revell 2012), specifying 'K' as the estimation method. For this and all further analyses using phylogenetic corrections, we used the phylogeny by Zheng and Wiens (2016). We matched the species in our dataset to the tips of the phylogeny with the 'treedata' function (package Geiger v.2.0.7: Pennell *et al.* 2014).

To quantify the variation in inner ear shape across our sample, we conducted a non-phylogenetic principal component analysis (PCA) using the 'gm.prcomp' function. To visualize this variation with respect to the phylogenetic relationships among taxa, we constructed a phylomorphospace using the first two axes of the PCA using the 'phylomorphospace' function in the R package PHYTOOLS (v.0.7.7: Revell 2012).

To assess and compare the effects of labyrinth size, skull shape, morpho-functional and ecological (substrate ecology) predictors on semicircular canal shape, we conducted phylogenetic Procrustes analyses of variance (ANOVA) and covariance (ANCOVA) tests using the 'procD.pgls' function (package GEOMORPH v.4.0.4: Adams *et al.* 2022). We considered the coefficient of determination (R^2) as a measure of the strength of a relationship and used it to compare models. As in Evers *et al.* (2022), we evaluated models iteratively, using significant variables from bivariate regressions for multiple regression models comparing explanatory variables, calculating significance and effect sizes from Type II sum of squares. Significant variables (or proxies thereof) from bivariate models were carried over into multivariate models, first assessing interactions and/or collinearity between pairs of predictors, and then carrying those that were significant into more complex models while removing collinear variables. We also tested these associations for centroid size, using the lm.rrpp function (package RRPP v.1.1.2: Collyer and Adams 2021), including a variance–covariance matrix of phylogenetic distances for the species in our sample, generated via the 'vcv.phylo' function in the package APE (v.5.4: Paradis and Schliep 2019). For these, we compared Akaike information criterion (AIC) weights of models using the 'model.comparison' function in RRPP, specifying log-likelihood as the estimation method.

To provide a further visualization of the shape differences between classes of limb reduction and substrate ecology groups, we conducted canonical variate analyses (CVA) using the 'CVA' function in the package MORPHO (v.2.10: Schlager 2017). Following Dickson *et al.* (2017), we used the first 34 axes from the PCA we conducted previously, representing 99% of semicircular canal shape variation, as input for the CVA. This ensured that the number of axes was lower than the number of specimens and reduced fluctuations in shape variance that might be attributed to error. We generated 90% confidence ellipses to visualize overlap across groups.

The workflow and code used for these analyses is based on Pollock *et al.* (2022) and Dickson *et al.* (2017). All these operations were performed in R (v.4.0.0: R Core Team 2022).

RESULTS

Semicircular canal shape variation in Australian sphenomorphine skinks

The first principal component axis (PC1) explains 27.81% of semicircular canal shape variation, the second (PC2) 15.49%, and the third (PC3) 11.61% (Fig. 3), cumulatively explaining more than half (55%) of the variation. PC1 correlates with distension of the labyrinth, meaning that semicircular canals become proportionally wider and rounder towards the positive end of the PC1 axis, but also remain more appressed towards the centre of the organ where they loop from its lateral to its medial side (Fig. 3A). Towards the negative end of the axis, the lateral semicircular canal becomes narrower and more dorsoventrally elevated in lateral view, and the curvatures of anterior and posterior semicircular canals bend inwards, increasing the ellipticity (Goyens 2019) (dorsoventral compression) of the axes (especially the anterior semicircular canal), and causing their medially directed loops to jut outwards and forwards (Fig. 3A). Moreover, the angle between the anterior and the posterior semicircular canal with respect to the crus commune increases from acute to orthogonal towards the positive end of the PC1 axis (Fig. 3A). PC2 correlates with the direction of compression of the lateral semicircular canal on the horizontal axis (going from posteromedial-anterolateral to anteromedial-posterolateral; Fig. 3A). The ventral angularity of the medially directed loops of the anterior and posterior semicircular canals, and the posterior shift of the position of the crus commune, both positively correlate with PC2 score (Fig. 3A). PC3 scales negatively with dorsoventral compression of the anterior and posterior semicircular canals, marked by a lower crus commune (Fig. 3B). PC3 also scales positively with an increase in the angle between the anterior and posterior semicircular canals (towards orthogonality), with a narrowing of the circumference of the posterior semicircular canal where it loops in the medial direction, and with a straightening of the lateral-facing loop of the lateral semicircular canal (Fig. 3B).

Visually, classes of limb reduction are placed along a gradient across PC1 (Fig. 4), in order from fully limbed to limbless from the negative to the positive end of the axis. The moderately limb-reduced category overlaps with the other three, and there is virtually no overlap between the fully limbed category and the limbless category over PC1. When these categories are included in a CVA, classes of limb reduction (especially the limbless category) are visually distinct, with the exception of moderately limb-reduced species, which appear to be contiguous both with highly limb-reduced species and, to a minor degree, fully limbed species (Fig. 5A).

Mapping substrate ecologies on the morphospace shows significant overlap between categories, with surface-dwelling (terrestrial) and humus categories being slightly more distinct. When considering a CVA with these categories, there is also significant overlap between categories, especially the sand and sandy soil categories, with surface-dwelling (terrestrial) and humus species being most distinct (Fig. 5B).

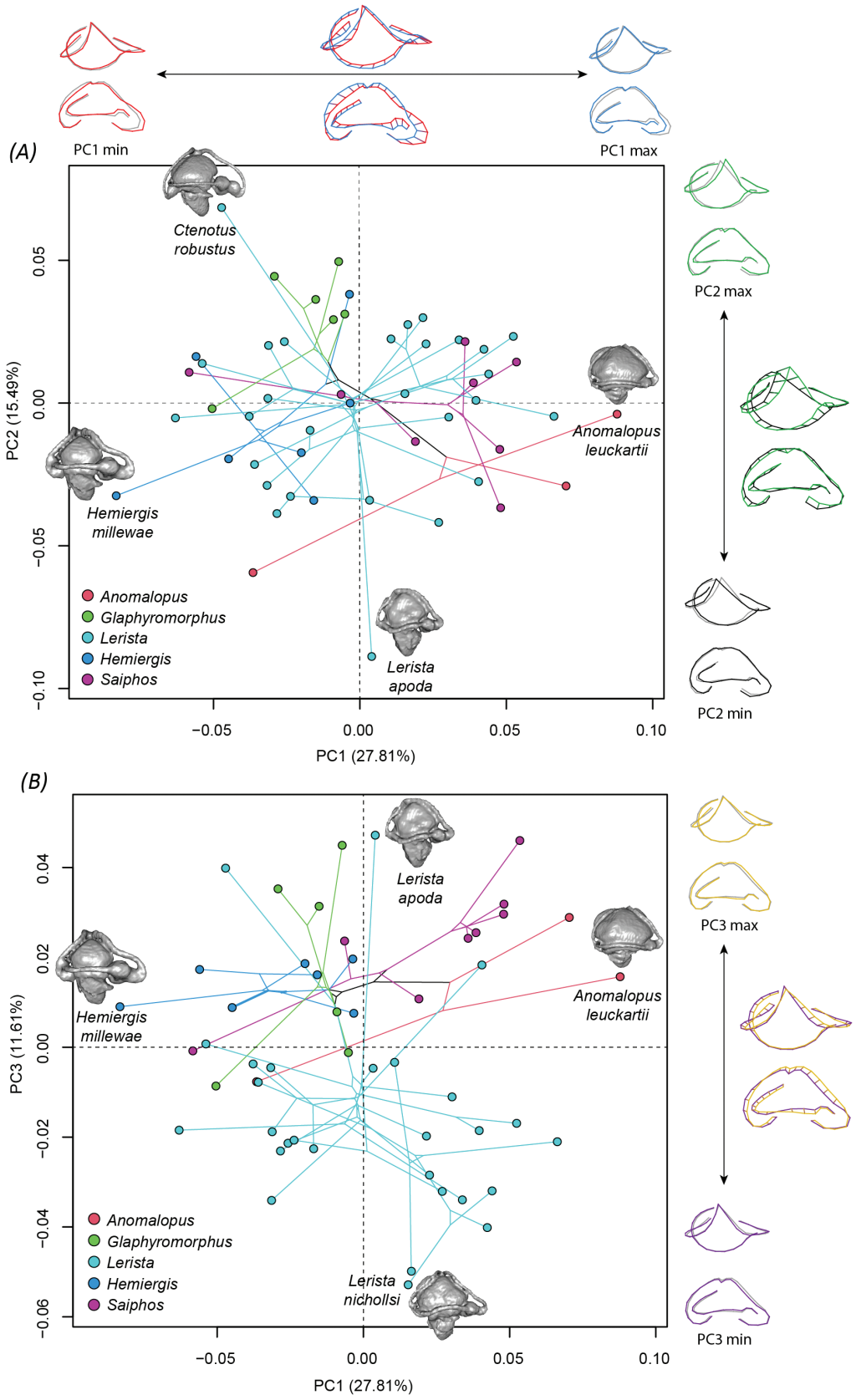

Figure 3. Phylomorphospace plots of semicircular canal shape in our skink dataset, showing (A) PC1 against PC2, and (B) PC1 against PC3, with focal clades shown in different colours. Proportions of shape variation explained by the axes are included in brackets. Maximum shape deformations for each axis are shown next to the PCAs, both in dorsal and lateral view (with anterior canal to the right, in colour), overlapped with mean shape (in grey). In-between, the maximum and minimum shape deformation are shown overlapped, in dorsal and lateral view.

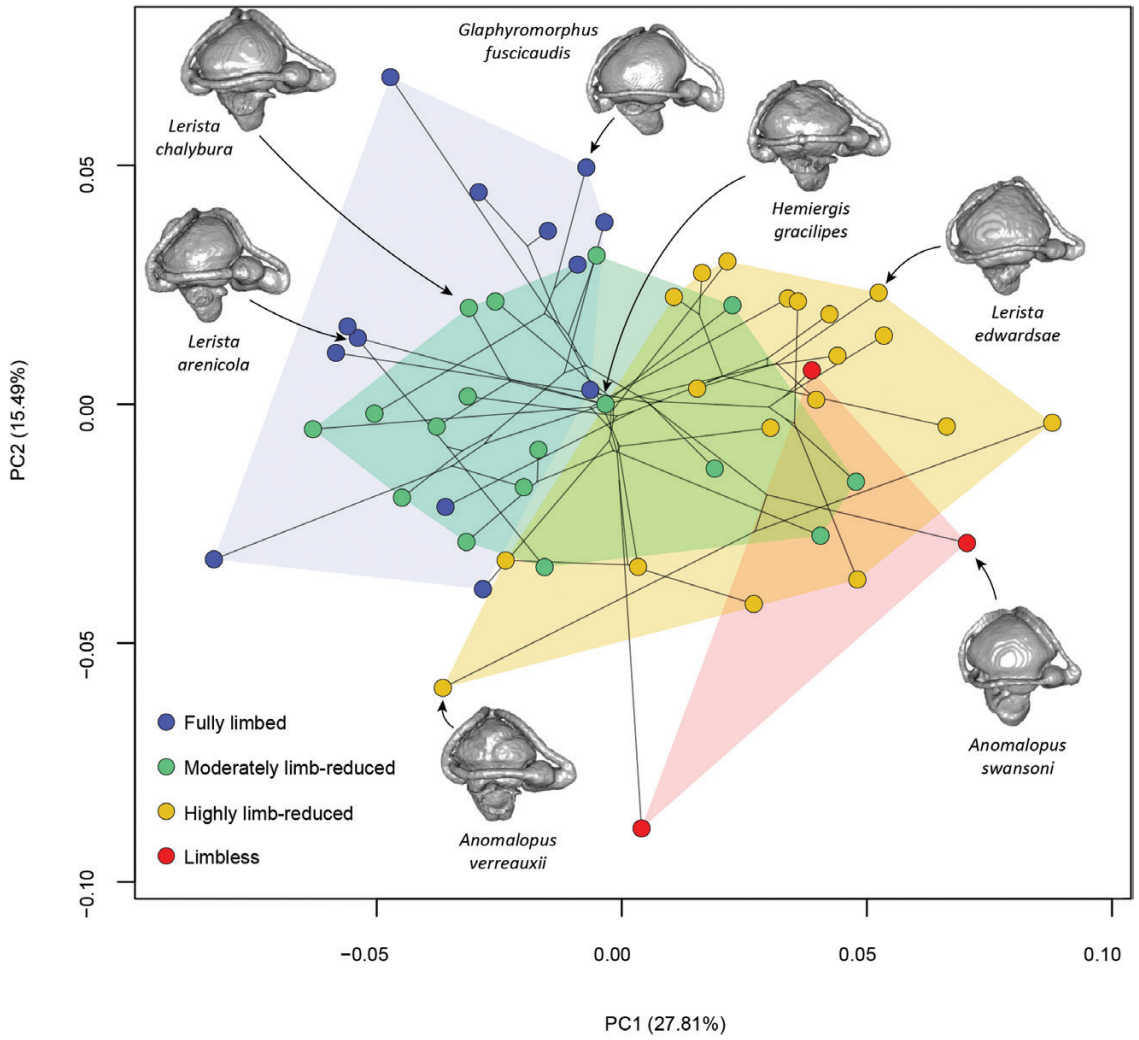

Figure 4. Phylomorphospace plot of the first two PC axes of semicircular canal shape variation. Proportions of shape variation explained by the axes are included in brackets. Each specimen is represented by a point, coloured by limb reduction status, and bounded by convex hulls.

Visually, both on PC1 and PC2 there is little evidence of phylogenetic clustering (Fig. 3A), but on PC3 it is evident for most clades (especially *Hemiergis*: Fig. 3B). Semicircular canal shape shows a moderate influence of phylogenetic history: we retrieved a significant phylogenetic signal K_{mult} ($K_{mult} = 0.69$, $P = 0.001$) in shape (as Procrustes coordinates) under the assumption of a Brownian motion evolutionary model (Revell *et al.* 2008).

Predictors of inner ear shape

The results of phylogenetic regressions based on Procrustes coordinates are summarized in Table 1. In bivariate regressions, we find significant associations between the semicircular canal shape of lizards in our sample and various parameters describing allometry, skull constraints, and general body shape. We retrieve limb status (a morpho-functional effect) as the strongest predictor of semicircular canal shape ($R^2 = 0.18$, $P = 0.001$), followed by saccular dimensions (height: $R^2 = 0.14$, $P = 0.001$; width at the top: $R^2 = 0.14$, $P = 0.001$; width at the bottom: $R^2 = 0.14$, $P = 0.001$; spherical volume: $R^2 = 0.14$, $P = 0.001$), centroid size ($R^2 = 0.11$, $P = 0.001$), and skull dimensions (height: $R^2 = 0.1$, $P = 0.001$; width: $R^2 = 0.11$, $P = 0.001$; length: $R^2 = 0.1$, $P = 0.001$). Semicircular canal shape weakly correlates with trunk elongation ($R^2 = 0.08$, $P = 0.001$), average head length ($R^2 = 0.06$, $P = 0.002$), and relative forelimb length [log(forelimb length/head length); $R^2 = 0.06$, $P = 0.004$](Table 1). No significant relationship is recovered between shape and relative hindlimb lengths, snout–vent length, limb disparity, or number of limb pairs (Table 1). The aspect ratio of skull elongation (length/width) has no detectable effect on semicircular canal shape ($R^2 = 0.03$, $P = 0.102$), and skull compression (height/width) has only moderate but significant effects on this feature ($R^2 = 0.05$, $P = 0.005$). Further, we find little evidence of direct associations between semicircular canal shape and ecomorphology (fossorial vs. surface-dwelling) or substrate ecology categories.

When significant variables (or proxies thereof) are used in multivariate models, testing the collinearity and strength of the interaction of pairs of predictors shows that the majority of variables related to structures in the skull (i.e. saccular volume, skull volume, and skull compression) are at least partially redundant. Additionally, limb status has significant interactions

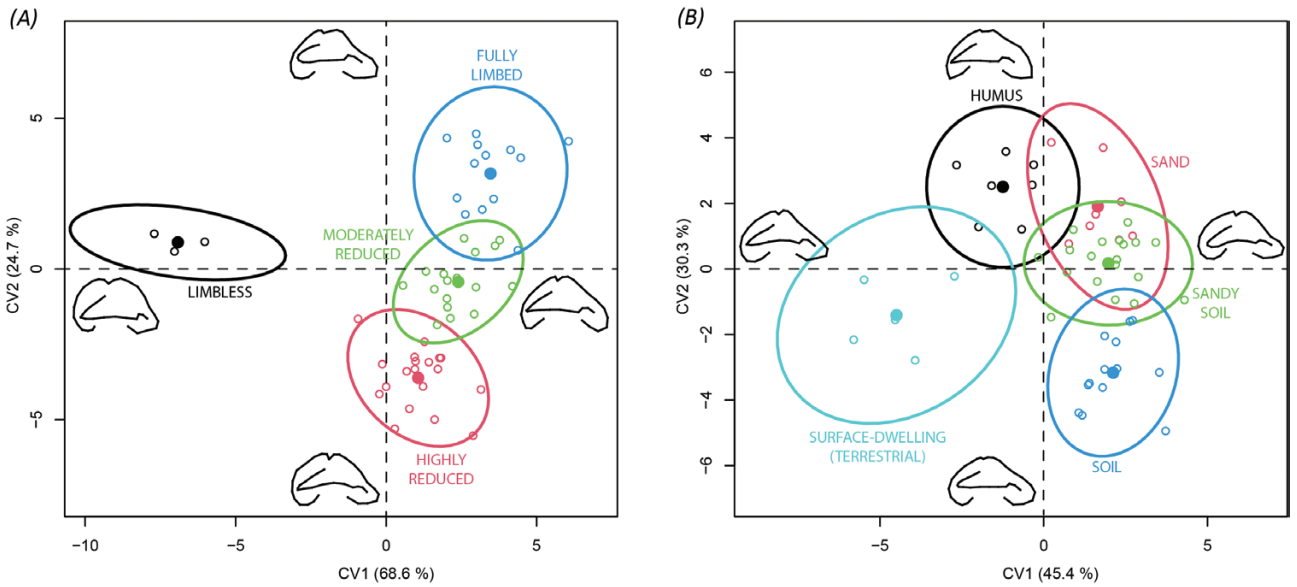

Figure 5. Canonical variate analysis (CVA) plots illustrating the first two axes of morphological variation in semicircular canal shape for (A) degrees of limb reduction, and (B) categories of substrate ecology. The mean of each group is shown in solid colour. Hollow points are specimens, coloured by category. Each group is enclosed in 90% confidence ellipses. Proportions of shape variation explained by the axes are included in brackets. Partial warps representing minima and maxima of each axis (in lateral view, with anterior canal facing right) are shown in black.

with the aforementioned skull variables ($R^2 < 0.09$), but its strongest interaction is with substrate ecology ($R^2 = 0.19$, $P = 0.032$).

Carrying these considerations over into more complex models, we find that aspect ratios of skull elongation and compression have negligible effects when included as covariates with most combinations of other predictors, indicating no significant effect of cranial constraints on semicircular canal shape. This is also true for trunk elongation, relative forelimb lengths, and head length. Additionally, although substrate ecology alone is not a significant predictor of shape, the interaction between it and limb status represents the most significant effect in our most supported models ($R^2 > 0.15$, $P = 0.001$). Indeed, all the explanatory models most supported by model comparisons ('~centroid size*limb status+substrate ecology*limb status', '~centroid size+substrate ecology*limb status', '~saccular volume+substrate ecology*limb status') include this interaction, with centroid size as a covariate (indicating this relationship is also allometric in nature). The interaction between centroid size, saccular volume, skull cuboid volume, and limb status is also featured in some of these highly supported models, showing the latter to be not completely independent from centroid size. The influence of skull volume (the variable carried over as a proxy for other skull dimensions) is greatly diminished (but still significant) when included in models together with either centroid size or saccular volume (or both). Both centroid size and saccular volume individually retain a similar significant effect (higher for the former) on inner ear shape in the most supported models. The general model support remains relatively high when they included together, but their relative influence on inner ear shape decreases, and so does model strength, showing them to be highly redundant.

Predictors of labyrinth centroid size

The results of phylogenetic regressions with centroid size are summarized in Table 2. Bivariate models retrieve centroid size as strongly positively correlated both with skull dimensions (height: $R^2 = 0.85$, $P = 0.001$; length: $R^2 = 0.87$, $P = 0.001$; width: $R^2 = 0.93$, $P = 0.001$; volume: $R^2 = 0.9$, $P = 0.001$), and saccular dimensions (height: $R^2 = 0.95$, $P = 0.001$; width at the top: $R^2 = 0.94$, $P = 0.001$; width at the bottom: $R^2 = 0.96$, $P = 0.001$; volume: $R^2 = 0.95$, $P = 0.001$) (Table 2). Centroid size also carries significant phylogenetic signal comparable with, if slightly higher than, that carried by semicircular canal shape ($K = 0.71$, $P = 0.024$).

Examining variables that describe different aspects of body shape, we find a significant association with limb status ($R^2 = 0.39$, $P = 0.001$), showing that highly limb-reduced species have comparably larger labyrinth sizes compared with limbless species, and fully limbed species have larger labyrinth sizes than moderately limb-reduced species. Centroid size does not significantly associate with number of limb pairs, or with the relative lengths of either pair of limbs, or with trunk elongation. It does, however, scale positively with head length (slope = 0.74, $R^2 = 0.67$, $P = 0.001$) and SVL (slope = 0.62, $R^2 = 0.5$, $P = 0.001$).

Labyrinth centroid size carries more ecological signal compared with shape, showing strong, direct associations with substrate ecology ($R^2 = 0.42$, $P = 0.001$), but not with ecomorph ($R^2 = 0.05$, $P = 0.117$). Labyrinth size is significantly higher in species from humus and in terrestrial species compared with all remaining substrate categories. Centroid size correlates positively (but weakly) with skull compression (slope = 0.99, $R^2 = 0.1$, $P = 0.027$) but not with skull elongation ($R^2 = 0.01$, $P = 0.444$) (Table 2).

Table 1. Results of the phylogenetic Procrustes regression models between semicircular canal shape and independent variables. All regressions are conducted with residual randomisation (RRPP). $N = 52$ for all models. Legend: shaded, $P < 0.05$; white, $P \geq 0.05$. Bivariate models are grouped by effect type

Model	Variable name	Effect	R-squared	F-statistic	Z-score	*P*-value	Model R-squared
~Skull compression (height/width)	Skull compression	Spatial constraint	0.053	2.821	2.574	0.005	0.053
~Skull elongation (length/width)	Skull elongation	Spatial constraint	0.032	1.672	1.335	0.102	0.032
~Skull height	Skull height	Allometric	0.098	5.443	4.118	0.001	0.098
~Skull length	Skull length	Allometric	0.104	5.806	4.208	0.001	0.104
Skull width	Skull width	Allometric	0.107	5.975	4.244	0.001	0.107
~Centroid size	Centroid size	Allometric	0.112	6.329	4.330	0.001	0.112
~Skull cuboid volume (length*width*height)	Skull cuboid volume	Allometric	0.104	5.809	4.224	0.001	0.104
~Limb disparity	Limb disparity	Morpho-functional	0.037	1.939	1.732	0.05	0.037
~Number of limb pairs	Number of limb pairs	Morpho-functional	0.051	1.307	0.885	0.186	0.051
~Forelimb length/Head length	Relative forelimb length	Morpho-functional	0.063	3.337	2.905	0.004	0.063
~Hindlimb length/Head length	Relative hindlimb length	Morpho-functional	0.032	1.639	1.243	0.126	0.032
~Snout-vent length	Snout-vent length	Morpho-functional	0.032	1.634	1.361	0.095	0.032
~Snout-vent length/Head length	Trunk elongation	Morpho-functional	0.081	4.436	3.740	0.001	0.081
~Head length	Head length	Morpho-functional	0.059	3.162	2.871	0.002	0.059
~Ecomorph	Ecomorph	Ecological	0.028	1.456	1.104	0.137	0.028
~Substrate type	Substrate type	Ecological	0.076	0.973	0.005	0.483	0.076
~Saccular height	Saccular height	Saccule	0.13937	8.0968	4.7753	0.001	0.139
~Saccular width at the top	Saccular width at the top	Saccule	0.14352	8.3787	4.8653	0.001	0.144
~Saccular width at the bottom	Saccular width at the bottom	Saccule	0.14428	8.4305	4.7989	0.001	0.144
~Saccular size (upper) (height*width at the top)	Saccular size (upper)	Saccule	0.144	8.410	4.850	0.001	0.144

Table 1. Continued

Model	Variable name	Effect	R-squared	F-statistic	Z-score	*P*-value	Model R-squared
~Saccular size (lower) (height*width at the bottom)	Saccular size (lower)	Saccule	0.143	8.328	4.796	0.001	0.143
Saccular spherical volume [calculated using (saccular width at the bottom)/2 as radius]	Saccular volume	Saccule	0.142	8.291	4.765	0.001	0.142
~Limb status	Limb status	Morpho-functional	0.17678	3.436	4.3996	0.001	0.177
~Centroid size + Skull compression + Limb status*Substrate ecology	Centroid size	Allometric	0.10143	7.5397	4.5169	0.001	0.472
	Skull compression	Spatial constraint	0.00978	0.7272	-0.577	0.722	
	Substrate ecology	Ecological	0.0554	1.0295	0.2445	0.397	
	Limb status	Morpho-functional	0.1175	2.9114	3.9858	0.001	
	Substrate ecology:Limb status	Interaction	0.18742	1.7414	3.3948	0.002	
~Substrate ecology*Limb status	Substrate ecology	Ecological	0.06276	0.9855	0.0526	0.483	0.413
	Limb status	Morpho-functional	0.16309	3.4143	4.0947	0.001	
	Substrate ecology:Limb status	Interaction	0.18724	1.47	1.9864	0.032	
~Saccular spherical volume*Limb status + Substrate ecology*Limb status	Saccular spherical volume	Saccule	0.11495	9.1278	4.9297	0.001	0.365
	Substrate ecology	Ecological	0.13611	3.6026	4.6928	0.426	
	Limb status	Morpho-functional	0.05152	1.0228	0.2109	0.001	
	Saccular spherical volume:Limb status	Interaction	0.06213	1.6444	2.1839	0.022	
	Substrate ecology:Limb status	Interaction	0.15029	1.7048	3.0974	0.003	
~Centroid size*Limb status + Substrate ecology*Limb status	Centroid size	Allometric	0.10002	7.6852	4.6985	0.001	0.518
	Substrate ecology	Ecological	0.05074	0.9747	-0.0386	0.523	
	Limb status	Morpho-functional	0.14953	3.8299	4.8443	0.001	
	Centroid size:Limb status	Interaction	0.06316	1.6176	2.059	0.019	

Table 1. Continued

Model	Variable name	Effect	R-squared	F-statistic	Z-score	*P*-value	Model R-squared
	Substrate ecology*Limb status	Interaction	0.15452	1.6961	2.9658	0.004	
~Limb status*Skull cuboid volume + Limb status*Substrate ecology + Saccular spherical volume + Centroid size	Limb status	Morpho-functional	0.07506	2.258	3.6818	0.001	0.44915
	Skull cuboid volume	Allometric	0.02337	2.1088	2.201	0.012	
	Substrate ecology	Ecological	0.0598	1.3491	1.78	0.04	
	Saccular volume	Saccule	0.06596	5.9524	4.6963	0.001	
	Centroid size	Allometric	0.03431	3.096	3.4111	0.001	
	Limb status:Skull cuboid volume	Interaction	0.05115	1.5387	2.0546	0.015	
	Limb status:Substrate ecology	Interaction	0.1395	1.7985	3.5223	0.002	
~Limb status*Substrate ecology + Saccular spherical volume + Centroid size	Limb status	Morpho-functional	0.07853	2.2478	3.7107	0.001	0.42844
	Substrate ecology	Ecological	0.06488	1.393	2.0167	0.026	
	Saccular volume	Saccule	0.07127	6.1204	5.0255	0.001	
	Centroid size	Allometric	0.0574	4.9288	4.5208	0.001	
	Limb status:Substrate ecology	Interaction	0.15636	1.6785	3.6607	0.001	
~Centroid size*Limb status + Saccular spherical volume*Limb status + Substrate ecology*Limb status	Centroid size	Allometric	0.05339	4.7992	4.4065	0.001	0.4734
	Limb status	Morpho-functional	0.07853	2.3529	3.9075	0.001	
	Saccular spherical volume	Saccule	0.06665	5.9913	4.8634	0.001	
	Substrate ecology	Ecological	0.05766	1.2958	1.4771	0.073	
	Centroid size:Limb status	Interaction	0.05304	1.5892	2.0919	0.016	
	Saccular spherical volume:Limb status	Interaction	0.0534	1.6001	2.1227	0.017	
	Substrate ecology:Limb status	Interaction	0.11073	1.6589	2.7112	0.003	
~Centroid size + Substrate ecology*Limb status	Limb status	Morpho-functional	0.14953	3.734	4.7403	0.001	0.50163

Table 1. Continued

Model	Variable name	Effect	R-squared	F-statistic	Z-score	*P*-value	Model R-squared
~Saccular spherical volume + Substrate ecology*Limb status	Substrate ecology	Ecological	0.05628	1.054	0.3876	0.355	0.49914
	Centroid size	Allometric	0.106	7.9413	4.6914	0.001	
	Substrate ecology:Limb status	Interaction	0.18982	1.7775	3.5552	0.002	
	Limb status	Morpho-functional	0.13611	3.5028	4.5774	0.001	
	Substrate ecology	Ecological	0.05823	1.1239	0.7339	0.244	
	Saccular spherical volume	Saccule	0.11988	9.2556	4.8687	0.001	
	Substrate ecology:Limb status	Interaction	0.18492	1.7846	3.7636	0.001	

The majority of these relationships do not persist when we include significant predictors from bivariate regressions in multivariate models. Saccular volume (used as a proxy of saccular dimensions) and skull cuboid volume (used as a proxy of skull dimensions) eclipse all other predictors in their explanatory power, as together they explain about 99% of the variation in centroid size (there is a very high collinearity between them, as both individually explain more than 90% of the variability in centroid size). Adding other significant predictors (i.e. substrate ecology and limb status) only marginally increases the coefficient of determination and lowers the AIC score of the model.

DISCUSSION

Functional correlates of vestibular shape and size

In this study, we aimed to disentangle the different types of signal carried by vestibular system morphology in a highly morphologically and ecologically variable group of lizards. The vestibular systems of our sampled Australian skinks exhibit substantial within-group variation in terms of both shape and size. We find that the most important predictor of semicircular canal shape is limb status—indicating classes of proportions of limb lengths to body length (SVL)—lending support to the locomotory hypothesis. This relationship is further highlighted in PC1, which also scales negatively with increases in relative limb lengths and positively with trunk elongation. The size of the inner ear also covaries with limb status, showing that these changes are allometric in nature. In squamates, the gradual shortening, miniaturization and eventual disappearance of limbs, and the elongation of the trunk is paired with evolutionary shifts from limb-propelled locomotion to axial-powered, undulatory locomotion, meaning that different limb proportions will correlate closely with locomotory mode (Leonard 1979, Morinaga and Bergmann 2020, Camaiti *et al.* 2021). These results thus point towards morpho-functional changes in inner ear labyrinth shape and size as a response to shifts in locomotory behaviour that accompany the reduction and/or loss of limbs.

The evolution of limb reduction is thought to be driven by the necessity to locomote more efficiently through cluttered settings such as thick vegetation and subterranean and interstitial habitats (Gans 1975, Camaiti *et al.* 2019, 2021, Macaluso *et al.* 2019). These conditions present unique opportunities for three-dimensional movement, leading to alterations in inner ear shape and size to better navigate these environments. Higher orthogonality between semicircular canals, a wider relative radius and a more circular shape of the lateral semicircular canal, and lower canal ellipticity—which in our sample correspond to the positive end of PC1 (Fig. 3)—have been linked with higher sensitivity to rotational head movements (Cox and Jeffery 2010, Goyens 2019). Changes in the shape and size of the semicircular canals affect sensitivity because they affect the speed of the endolymph flow through them, and thus the speed at which hair cells are stimulated, resulting in variation of the threshold of detection of mechanical stimuli from different patterns of movement (Oman *et al.* 1987, Muller 1994, Goyens 2019). In turn, increases in sensitivity were found to correlate with greater agility and manoeuvrability in vertebrate clades, including mammals (Cox and Jeffery 2008, 2010, Grohé *et al.* 2016) and

Table 2. Results of the phylogenetic regression models between semicircular canal size (as centroid size) and independent variables. All regressions were conducted with residual randomisation (RRPP). $N = 52$ for all models. Legend: shaded, $P < 0.05$; white, $P \geq 0.05$. Bivariate models are grouped by effect type. AIC values are indicated for each model

Model	Variable name	Effect	R-squared	F statistic	Z score	*P*-value	Model R-squared	AIC
~Skull compression (height/width)	Skull compression	Spatial constraint	0.097	5.400	1.333	0.027	0.097	34.950
~Skull elongation (length/width)	Skull elongation	Spatial constraint	0.012	0.622	0.304	0.444	0.012	39.640
~Skull height	Skull height	Allometric	0.853	289.308	3.207	0.001	0.853	-59.287
~Skull length	Skull length	Allometric	0.871	338.572	3.165	0.001	0.871	-66.337
~Skull width	Skull width	Allometric	0.934	704.164	3.737	0.001	0.934	-100.820
~Skull cuboid volume (length*width*height)	Skull cuboid volume	Allometric	0.902	460.260	3.538	0.001	0.902	-80.504
~Limb status	Limb status	Morpho-functional	0.393	10.358	2.665	0.001	0.393	18.328
~Limb disparity	Limb disparity	Morpho-functional	0.058	3.060	1.094	0.099	0.058	37.197
~Number of limb pairs	Number of limb pairs	Morpho-functional	0.020	0.500	-0.046	0.584	0.020	41.236
~Forelimb length/Head length	Relative forelimb length	Morpho-functional	0.027	1.392	0.720	0.246	0.027	38.859
~Hindlimb length/Head length	Relative hindlimb length	Morpho-functional	0.002	0.103	-0.428	0.752	0.002	40.180
~Snout-vent length	Snout-vent length	Morpho-functional	0.499	49.890	2.345	0.001	0.499	4.300
~Snout-vent length/Head length	Trunk elongation	Morpho-functional	0.010	0.514	0.294	0.45	0.010	39.750
~Head length	Head length	Morpho-functional	0.666	99.600	2.610	0.001	0.666	16.700
~Ecomorph	Ecomorph	Ecological	0.052	2.721	1.059	0.117	0.052	37.530
~Substrate ecology	Substrate ecology	Ecological	0.416	8.354	2.818	0.001	0.416	18.358
~Saccular height	Saccular height	Saccule	0.947	897.950	3.615	0.001	0.947	-112.710
~Saccular width at the top	Saccular width (upper)	Saccule	0.943	830.040	3.542	0.001	0.943	-108.846
~Saccular width at the bottom	Saccular spherical volume	Saccule	0.963	1301.300	3.872	0.001	0.963	-131.148
~Saccular size (upper) (height*width at the top)	Saccular size (upper)	Saccule	0.959	1180.466	3.649	0.001	0.959	-126.276
~Saccular size (lower) (height*width at the bottom)	Saccular size (lower)	Saccule	0.964	1325.984	3.898	0.001	0.964	-132.088

Table 2. Continued

Model	Variable name	Effect	R-squared	F statistic	Z score	*P*-value	Model R-squared	AIC
~Saccular spherical volume	Saccular spherical volume	Saccule	0.947	894.720	3.458	0.001	0.947	-134.626
Saccular spherical volume*Substrate ecology	Saccular spherical volume	Saccule	0.5597	1120.838	3.8126	0.001	0.98	-144.668
	Substrate ecology	Ecological	0.00986	4.9354	2.1726	0.003		
	Saccular spherical volume:Substrate ecology	Interaction	0.00378	1.89	1.0787	0.125		
~Saccular spherical volume*Limb status	Saccular spherical volume	Saccule	0.58597	1560.338	3.6454	0.001	0.99	-161.067
	Limb status	Morpho-functional	0.01356	12.0377	2.7884	0.001		
	Saccular spherical volume:Limb status	Interaction	0.00452	4.0129	1.7927	0.015		
Saccular spherical volume + Head length	Saccular spherical volume	Saccule	0.310523	641.953	3.5988	0.001	0.98	-152.308
	Head length	Morpho-functional	0.010905	22.544	2.0443	0.001		
Saccular spherical volume + Skull cuboid volume	Saccular spherical volume	Saccule	0.02136	78.6138	2.3748	0.001	0.99	-182.561
	Skull cuboid volume	Allometric	0.084743	311.8922	2.91514	0.001		
Saccular spherical volume + Skull cuboid volume*Substrate ecology	Saccular spherical volume	Saccule	0.059045	314.9493	3.2388	0.001	0.99	-194.865
	Skull cuboid volume	Allometric	0.013373	71.3332	2.5036	0.001		
	Substrate ecology	Ecological	0.001872	2.4958	1.3467	0.07		
	Skull cuboid volume:Substrate ecology	Interaction	0.003689	4.9192	2.2298	0.002		

lizards (Dickson *et al.* 2017, Vasilopoulou-Kampitsi 2019b). As our analyses take phylogeny into account, and the effects of cranial constraints on inner ear shape are small, this points towards an adaptive specialization of inner ear shape and size in these lizards. Complex locomotory behaviours, including arboreality and fossoriality, have been linked with shapes indicating increased sensitivity of the vestibular system in amphibians and lizards (Dickson *et al.* 2017, Capshaw *et al.* 2019). It must be noted, however, that these conclusions are contradicted by other studies (Vasilopoulou-Kampitsi *et al.* 2019b) linking sensitivity with simple environments instead of complex ones. The correlation with limb reduction status appear to support the former association, showing that, as limb-reduced body shapes tend to require navigation in complex three-dimensional mediums, concomitant changes occur in the semicircular canals that increase ear sensitivity. This would also imply that more 'limbed' skinks would have less sensitive inner ears compared with their limb-reduced relatives.

The wider radius of the semicircular canals (which increases with PC1, Fig. 3) may also be indirectly caused by the abnormal expansion of the saccule, which is common among fossorial and semifossorial forms in squamates (Yi and Norell 2015, Palci *et al.* 2017, Capshaw *et al.* 2019, Yi 2022). Indeed, this appears to be supported by our finding that vestibular dimensions (as vestibular volume), while being also in large part explained by allometry (being collinear with centroid size: see Table 2), are one of the largest effects explaining semicircular canal shape. This is contrasted with the 'external' spatial constraints delimited by skull dimensions (as in: Evers *et al.* 2022), which in our models are found to have a comparably low to no influence on semicircular canal morphology (Table 1; see second part of the discussion), the significant relationship with vestibular expansion can be interpreted as evidence of 'internal' spatial constraints. As the saccule can perceive linear accelerations and gravity, its enlargement may represent a functional adaptation for a lizard to assess its orientation and directionality of movement within a complex environment, like the cluttered settings that are considered among the strongest environmental drivers of limb reduction (Gans 1975, Camaiti *et al.* 2019). Moreover, the saccule is known to possess auditory capabilities as its hair cells are able to detect sounds and vibrations (Capshaw *et al.* 2022), complementing the functions of the lagena (the cochlea of lizards: Evans 2016). Saccular expansion has been linked to better detection of lower-frequency vibrations—as opposed to airborne sounds—in fossorial (and limbless) tetrapods like caecilians (Maddin and Sherratt 2014) and snakes (Yi and Norell 2015, Yi 2022). Thus, auditory capabilities may also represent a driver of the absolute and relative (compared to skull and body size) increase in the size of the saccule. As the interaction term between limb status and vestibular expansion is also a significant predictor of semicircular canal shape in our models—albeit, much less relevant compared with the interaction between body shape and ecology—this may indicate that vestibular expansion also follows changes in body shape, and thus locomotory performance. Overall, these results appear to validate the hypothesis that the intrinsic biomechanical (and largely allometric) pressures of saccular expansion, which in our analyses are independent from cranial constraints, represent a driver of semicircular canal shape, together with the direct selective pressures of locomotion.

Finally, the finding that both semicircular canal shape and size carry ecological signal brings further validation of the ecomorphological hypothesis, with the corollary that associations with shape are significant only in relation to limb status—and hence, locomotion. Changes in body shapes associated with varying locomotory strategies have been shown to differ across substrate niches in fossorial lizards (Morinaga and Bergmann 2020, Stepanova and Bauer 2021, Camaiti *et al.* 2023). The significant interaction between locomotory strategy (as a function of body shape variation) and substrate ecology explaining most inner ear shape variation implies that the differential interactions between body shapes and distinct environments could require varying sensory needs, which would then induce alterations in vestibular shape and size. For instance, humus-dwellers—which in our analyses often come up as distinct both in shape and size from other categories—experience different conditions from substrate-swimmers in terms of how, and how quickly, they move within their substrate (i.e. friable soils behave like fluids and facilitate fast locomotion, while soils rich in organic aggregates require forced displacement of material: Attum *et al.* 2007, Crofts and Summers 2011, Camaiti *et al.* 2023). As studies like Camaiti *et al.* (2023) have shown, these distinct conditions consistently associate with particular body morphologies in limb-reduced lizards, in that each is more adapted for efficient locomotion through a given medium (i.e. high limb disparity and head miniaturisation in sand-dwellers, as opposed to equal limb lengths and larger heads in humus-dwellers). These different conditions and associated locomotory strategies may select for distinct sensory capabilities in terms of sensitivity and sound detection. Further studies are needed to parse the sensory implications of semicircular canal shape and size changes depending on locomotory capabilities and substrate type in fossorial animals, and how they might affect the physical properties of balance and sound detection. As these associations are merely based on observations of morphology quantified through changes across PC axes, direct physiological and locomotory experiments are required to validate functional explanations.

Spatial constraints, allometry, and phylogenetic signal

Our analyses show that spatial constraints resulting from modifications of skull shape exert only a relatively small influence on semicircular canal shape, which becomes negligible compared with other factors such as locomotion, allometry, and ecology. Excluding the effects of spatial allometry, inner ear shape and size correlate only weakly with variations in the aspect ratio of skull compression (height/width), a relationship that does not change even when including ecology, centroid size, and locomotion as covariates. This implies at least a partial refutation of the 'spatial constraints' hypothesis for our sample. The skull shape of lizards can be expected to change depending on characteristics of the environment and on phylogenetic history, and as the inner ear is housed within the skull, this introduces the possibility that the influence of these factors may indirectly affect semicircular canal shape as well. Studies like Goyens (2019) have shown that, compared with mammals, the flattening experienced by squamate skulls tends to have severe implications on semicircular canal shape, dramatically increasing their ellipticity (dorsoventral compression) and decreasing their sensitivity as a result. In

our sample, this does not seem to be the case, as, for example, the pattern of shape change that is observable in PC2 remains weak compared with allometry, and does not seem to particularly affect dorsoventral eccentricity but only deformations in the horizontal plane. In contrast to the arboreal or surface-dwelling taxa considered in Goyens (2019), fossorial and semifossorial forms (the majority of our sample) tend to have conical or cylindrical skulls with low diameters and less pronounced skull protrusions (such as paraoccipital processes and sphenooccipital tubercles: Greer and Cogger 1985; Hutchinson *et al.* 2021) to lower lateral drag and facilitate head-first substrate penetration (Roscito and Rodrigues 2010, Kazi and Hipsley 2018, Stepanova and Bauer 2021). In the light of this, our results point to the absence of significant morpho-functional trade-offs between skull shape and semicircular canal shape as skinks evolved limb reduction and fossoriality, and that the existence of these trade-offs may be largely clade-dependent. As the evolutionary tendency towards head miniaturization is common as limb reduction and fossoriality become more pronounced (Rieppel 1984, Lee 1998, de Barros *et al.* 2011, 2021, Gurgis *et al* 2021), this also suggests that inner ear shape is not particularly affected, as skull dimensions tend to scale proportionally in all directions. One possible limitation of these considerations is the fact that our sample is largely comprised of skinks with similar skull height and width, as opposed to very flattened skull shapes. While this is likely due to skinks tending to have cylindrical body and conical head shapes even when not limb-reduced (Zug *et al.* 2001), it may suggest that larger samples of comparative material including more fully limbed species are required to parse these patterns.

In terms of spatial allometry, skull cuboid volume and individual skull dimensions correlate strongly ($R^2 > 0.9$) with centroid size. The slightly negative allometric relationship between centroid size and skull cuboid volume (slope = 0.301, keeping in mind that isometry would produce a slope of 0.33 for regressions between linear and cube variables) indicates that inner ear size is relatively smaller in larger skulls, validating the findings of previous studies (Dickson *et al.* 2017, Vasilopoulou-Kampitsi 2019a). Given its high correlation with centroid size, skull cuboid volume essentially has the same relationships with semicircular canal shape, which, therefore, again reflects the significant shape-size allometry we detected in the semicircular canal. In our most supported models explaining semicircular canal shape, the interaction between skull volume and centroid size becomes non-significant when considering them together (Table 2); this implies that any existing spatial trade-off between the size of the inner ears and that of the skull only exerts a comparably small influence on semicircular canal shape. While skull miniaturization has been identified as a factor influencing inner ear shape in some fossorial taxa like snakes (Olori 2010), this does not appear to be the case for fossorial skinks, which is also validated by our finding that cranial constraints are not influential in determining inner ear shape.

When examining the role of phylogenetic history in determining semicircular canal shape, we find evidence of significant and moderate phylogenetic signal ($K = 0.69$), suggesting that historical influences play a role in determining what morphologies are allowed by the constraints of evolutionary development. As this signal is lower than expected under a Brownian motion model of trait evolution (Revell *et al.* 2008), this also indicates some degree of morphological convergence across our sample, which is evident from the many overlapping branches in the phylomorphospace (Figs 2–4). Indeed, as different lineages of skinks have convergently evolved limb reduction (albeit probably following different trajectories: Bergmann and Morinaga 2019, Camaiti *et al.* 2023), and given the association we find between limb reduction and semicircular canal shape, this may also reflect on the evolution of inner ear morphologies. Including larger samples of taxa from different lineages and body morphologies may increase our ability to detect whether these patterns are convergent or just an effect of incomplete sampling.

CONCLUSION

When examining semicircular canal shape in sphenomorphine skinks, our results validate a locomotory hypothesis, given that we retrieve limb status (the degree of limb reduction, indicative of general locomotory mode) as the main explanatory variable of shape. As limb-propelled locomotory strategies transition to undulatory, axial-propelled locomotion, several aspects of the shape of the labyrinth system change accordingly, probably reflecting shifts in the sensory needs associated with that locomotory strategy. The significant interaction with substrate ecology reinforces the idea that, as limb reduction and undulatory locomotion often associate with complex, three-dimensional settings (i.e. the substrate), these changes may become necessary to navigate these environments more efficiently. While physiological and locomotory experiments are required to validate morpho-functional hypotheses, the patterns of morphological convergence we observe across different clades of skinks support the use of labyrinth shape as a consistent predictor of locomotory strategies and the associated environmental context.

SUPPLEMENTARY DATA

Supplementary data is available at *Zoological Journal of the Linnean Society* Journal online.

ACKNOWLEDGEMENTS

We wish to thank Dr Jay Black for the technical expertise for acquiring our scans, and the reviewers for kindly reviewing our manuscript. This project was supported by the Holsworth Wildlife Research Endowment (Equity Trustees Charitable Foundation and the Ecological Society of Australia; to M.C.), the Monash-Museums Victoria Robert Blackwood scholarship (to M.C.), an Australian Research Council Linkage Project grant (LP170100012; to D.G.C., A.R.E., and M.N.H.), an Australian Research Council Future Fellowship grant (FT200100108; to D.G.C.), and a Discovery Early Career Researcher Award (DECRA: DE180100629, to C.A.H.). The authors declare no conflict of interest.

CONFLICT OF INTEREST

None declared.

DATA AVAILABILITY

The data underlying this article are available in the article and in its online supplementary material. The R code and additional files used

to reproduce the analyses are accessible on the Bridges repository at https://doi.org/10.26180/22817171.

REFERENCES

Adams D, Collyer M, Kaliontzopoulou A *et al. geomorph: Software for Geometric Morphometric Analyses. R Package Version 4.0.4*, 2022. https://cran.r-project.org/package=geomorph (22 October 2022, date last accessed)

Attum O, Eason P, Cobbs G. Morphology, niche segregation, and escape tactics in a sand dune lizard community. *Journal of Arid Environments* 2007;**68**:564–73.

de Barros FC, Herrel A, Kohlsdorf T. Head shape evolution in Gymnophthalmidae: does habitat use constrain the evolution of cranial design in fossorial lizards? *Journal of Evolutionary Biology* 2011;**24**:2423–33.

de Barros FC, Grizante MB, Zampieri FA *et al*. Peculiar relationships among morphology, burrowing performance and sand type in two fossorial microteiid lizards. *Zoology* 2021;**144**:125880.

Benson RB, Starmer-Jones E, Close RA *et al*. Comparative analysis of vestibular ecomorphology in birds. *Journal of Anatomy* 2017;**231**:990–1018.

Bergmann PJ, Morinaga G. The convergent evolution of snake-like forms by divergent evolutionary pathways in squamate reptiles. *Evolution* 2019;**73**:481–96.

Berlin JC, Kirk EC, Rowe TB. Functional implications of ubiquitous semicircular canal non-orthogonality in mammals. *PLoS One* 2013;**8**:e79585.

Bronzati M, Benson RB, Evers SW *et al*. Deep evolutionary diversification of semicircular canals in archosaurs. *Current Biology* 2021;**31**:2520–2529.e6.

Camaiti M, Villa A, Wencker LC *et al*. Descriptive osteology and patterns of limb loss of the European limbless skink *Ophiomorus punctatissimus* (Squamata, Scincidae). *Journal of Anatomy* 2019;**235**:313–45.

Camaiti M, Evans AR, Hipsley CA *et al*. A farewell to arms and legs: a review of limb reduction in squamates. *Biological Reviews* 2021;**96**:1035–50.

Camaiti M, Evans AR, Hipsley CA *et al*. A database of the morphology, ecology and literature of the world's limb-reduced skinks. *Journal of Biogeography* 2022;**49**:1397–406.

Camaiti M, Evans AR, Hipsley CA *et al*. Macroecological and biogeographical patterns of limb reduction in the world's skinks. *Journal of Biogeography* 2023;**50**:428–40.

Capshaw G, Soares D, Carr CE. Bony labyrinth morphometry reveals hidden diversity in lungless salamanders (Family Plethodontidae): Structural correlates of ecology, development, and vision in the inner ear. *Evolution* 2019;**73**:2135–50.

Capshaw G, Christensen-Dalsgaard J, Carr CE. Hearing without a tympanic ear. *Journal of Experimental Biology* 2022;**225**:jeb244130.

Collyer ML, Adams DC. *RRPP: Linear Model Evaluation with Randomized Residuals in a Permutation Procedure, R Package v.1.1.2*, 2021. https://cran.r-project.org/package=RRPP (15 September 2022, date last accessed)

Costeur L, Grohé C, Aguirre-Fernández G *et al*. The bony labyrinth of toothed whales reflects both phylogeny and habitat preferences. *Scientific Reports* 2018;**8**:1–6.

Cox PG, Jeffery N. Geometry of the semicircular canals and extraocular muscles in rodents, lagomorphs, felids and modern humans. *Journal of Anatomy* 2008;**213**:583–96.

Cox PG, Jeffery N. Semicircular canals and agility: the influence of size and shape measures. *Journal of Anatomy* 2010;**216**:37–47.

Crofts SB, Summers AP. Swimming in the Sahara. *Nature* 2011;**472**:177–8.

David R, Bronzati M, Benson RB. Comment on 'The early origin of a birdlike inner ear and the evolution of dinosaurian movement and vocalization'. *Science* 2022;**376**:eabl6710.

Dickson BV, Sherratt E, Losos JB *et al*. Semicircular canals in Anolis lizards: ecomorphological convergence and ecomorph affinities of fossil species. *Royal Society Open Science* 2017;**4**:170058.

Ekdale EG. Form and function of the mammalian inner ear. *Journal of Anatomy* 2016;**228**:324–37.

Evans SE. The lepidosaurian ear: variations on a theme. In: Clack JA, Fay RR, Popper AN (eds), *Evolution of the Vertebrate Ear*. Cham: Springer, 2016, 245–84.

Evers SW, Joyce WG, Choiniere JN *et al*. Independent origin of large labyrinth size in turtles. *Nature Communications* 2022;**13**:1–15.

Gans C. Tetrapod limblessness: evolution and functional corollaries. *American Zoologist* 1975;**15**:455–67.

Garland T Jr, Losos JB. Ecological morphology of locomotor performance in Squamate reptiles. In: Wainwright PC, Reilly SM (eds), *Ecological Morphology: Integrative Organismal Biology*. Chicago and London: The University of Chicago Press, 1994, 240–302.

Gonzales LA, Malinzak MD, Kay RF. Intraspecific variation in semicircular canal morphology—A missing element in adaptive scenarios? *American Journal of Physical Anthropology* 2019;**168**:10–24.

Goyens J. High ellipticity reduces semi-circular canal sensitivity in squamates compared to mammals. *Scientific Reports* 2019;**9**:1–8.

Goyens J, Aerts P. Head stabilisation in fast running lizards. *Zoology* 2018;**127**:114–20.

Greer AE. *The Biology and Evolution of Australian Lizards*. Chipping Norton, New South Wales: Surrey Beatty and Sons, 1989.

Greer AE, Cogger HG. Systematics of the reduce-limbed and limbless skinks currently assigned to the genus Anomalopus (Lacertilia: Scincidae). *Records of the Australian Museum* 1985;**37**:11-54.

Grohé C, Tseng ZJ, Lebrun R *et al*. Bony labyrinth shape variation in extant Carnivora: a case study of Musteloidea. *Journal of Anatomy* 2016;**228**:366–83.

Gurgis GP, Daza JD, Brennan IG *et al*. Ecomorphometric analysis of diversity in cranial shape of pygopodid geckos. *Integrative Organismal Biology* 2021;**3**:obab013.

Hanson M, Hoffman EA, Norell MA *et al*. The early origin of a birdlike inner ear and the evolution of dinosaurian movement and vocalization. *Science* 2021;**372**:601–9.

Hutchinson MN, Couper P, Amey A *et al*. Diversity and systematics of limbless skinks (*Anomalopus*) from eastern Australia and the skeletal changes that accompany the substrate swimming body form. *Journal of Herpetology* 2021;**55**:361–84.

Kazi S, Hipsley CA. Conserved evolution of skull shape in Caribbean head-first burrowing worm lizards (Squamata: Amphisbaenia). *Biological Journal of the Linnean Society* 2018;**125**:14–29.

Lee MS. Convergent evolution and character correlation in burrowing reptiles: towards a resolution of squamate relationships. *Biological Journal of the Linnean Society* 1998;**65**:369–453.

Le Guilloux M, Miralles A, Measey J *et al*. Trade-offs between burrowing and biting force in fossorial scincid lizards? *Biological Journal of the Linnean Society* 2020;**130**:310–9.

Leonard CJ. A functional morphological study of limb regression in some southern African species of Scincidae (Reptilia: Sauria). *Ph.D. dissertation*, University of Cape Town, 1979.

Macaluso L, Carnevale G, Casu R *et al*. Structural and environmental constraints on reduction of paired appendages among vertebrates. *Biological Journal of the Linnean Society* 2019;**128**:473–85.

Maddin HC, Sherratt E. Influence of fossoriality on inner ear morphology: insights from caecilian amphibians. *Journal of Anatomy* 2014;**225**:83–93.

Malinzak MD, Kay RF, Hullar TE. Locomotor head movements and semicircular canal morphology in primates. *Proceedings of the National Academy of Sciences* 2012;**109**:17914–9.

Morinaga G, Bergmann PJ. Evolution of fossorial locomotion in the transition from tetrapod to snake-like in lizards. *Proceedings of the Royal Society B* 2020;**287**:20200192.

Muller M. Semicircular duct dimensions and sensitivity of the vertebrate vestibular system. *Journal of Theoretical Biology* 1994;**167**:239–56.

Olori JC. Digital endocasts of the cranial cavity and osseous labyrinth of the burrowing snake *Uropeltis woodmasoni* (Alethinophidia: Uropeltidae). *Copeia* 2010;**2010**:14–26.

Oman CM, Marcus EN, Curthoys IS. The influence of semicircular canal morphology on endolymph flow dynamics. An anatomically descriptive mathematical model. *Acta Oto-laryngologica* 1987;**103**:1–13.

Palci A, Hutchinson MN, Caldwell MW *et al*. The morphology of the inner ear of squamate reptiles and its bearing on the origin of snakes. *Royal Society Open Science* 2017;**4**:170685.

Paradis E, Schliep K. ape 5.0: an environment for modern phylogenetics and evolutionary analyses in R. *Bioinformatics* 2019;**35**:526–8.

Pennell M, Eastman J, Slater G *et al*. geiger v.2.0: an expanded suite of methods for fitting macroevolutionary models to phylogenetic trees. *Bioinformatics* 2014;**30**:2216–8.

Pollock TI, Hocking DP, Evans AR. The killer's toolkit: remarkable adaptations in the canine teeth of mammalian carnivores. *Zoological Journal of the Linnean Society* 2022;**196**:1138–55.

Rabbitt RD, Damiano ER, Grant JW. Biomechanics of the semicircular canals and otolith organs. In: Highstein SM, Fay RR, Popper AN (eds), *The Vestibular System*. New York, NY: Springer, 2004, 153–201.

Ramprashad F, Landolt JP, Money KE *et al*. Comparative morphometric study of the vestibular system of the vertebrata: Reptilia, Aves, Amphibia, and Pisces. *Acta Oto-laryngologica. Supplementum* 1986;**427**:1–42.

R Core Team. *R: A Language and Environment for Statistical Computing*. Vienna, Austria: R Foundation for Statistical Computing, 2022. https://www.R-project.org/ (1 October 2022, date last accessed)

Revell LJ. phytools: an R package for phylogenetic comparative biology (and other things). *Methods in Ecology and Evolution* 2012;**2**:217–23.

Revell LJ, Harmon LJ, Collar DC. Phylogenetic signal, evolutionary process, and rate. *Systematic Biology* 2008;**57**:591–601.

Rieppel O. Miniaturization of the lizard skull: its functional and evolutionary implications. *Symposia of the Zoological Society of London* 1984;**52**:503–20.

Roscito JG, Rodrigues MT. Comparative cranial osteology of fossorial lizards from the tribe Gymnophthalmini (Squamata, Gymnophthalmidae). *Journal of Morphology* 2010;**271**:1352–65.

Schlager S. Morpho and Rvcg–shape analysis in R: R-packages for geometric morphometrics, shape analysis and surface manipulations. In: Zheng G, Li S, Szekely G (eds), *Statistical Shape and Deformation Analysis*. London: Academic Press, 2017, 217–56.

Shea GM. Nomenclature of supra-generic units within the Family Scincidae (Squamata). *Zootaxa* 2021;**5067**:301–51.

Skinner A, Hutchinson MN, Lee MS. Phylogeny and divergence times of Australian Sphenomorphus group skinks (Scincidae, Squamata). *Molecular Phylogenetics and Evolution* 2013;**69**:906–18.

Spoor F, Zonneveld F. Morphometry of the primate bony labyrinth: a new method based on high-resolution computed tomography. *Journal of Anatomy* 1995;**186**:271.

Spoor F, Garland T Jr, Krovitz G *et al*. The primate semicircular canal system and locomotion. *Proceedings of the National Academy of Sciences* 2007;**104**:10808–12.

Steinhausen W. Über die Bobachtungen der Cupula in den Bogengangsampullen des Labyrinthes des lebenden Hechts. *Plägers Archiv* 1933;**232**:500–12.

Stepanova N, Bauer AM. Phylogenetic history influences convergence for a specialized ecology: comparative skull morphology of African burrowing skinks (Squamata; Scincidae). *BMC ecology and evolution* 2021;**21**:1–53.

Uetz P, Freed P, Aguilar R *et al*. *The Reptile Database*, 2022. http://www.reptile-database.org (21 November 2022, date last accessed).

Vanhooydonck B, Boistel R, Fernandez V *et al*. Push and bite: trade-offs between burrowing and biting in a burrowing skink (*Acontias percivali*). *Biological Journal of the Linnean Society* 2011;**102**:91–9.

Vasilopoulou-Kampitsi M, Goyens J, Baeckens S *et al*. Habitat use and vestibular system's dimensions in lacertid lizards. *Journal of Anatomy* 2019a;**235**:1–14.

Vasilopoulou-Kampitsi M, Goyens J, Van Damme R *et al*. The ecological signal on the shape of the lacertid vestibular system: simple versus complex microhabitats. *Biological Journal of the Linnean Society* 2019b;**127**:260–77.

Wever EG. *The Reptilian Ear: Its Structure and Function*. New Jersey: Princeton University Press, 1978.

Wiens JJ, Slingluff JL. How lizards turn into snakes: a phylogenetic analysis of body-form evolution in anguid lizards. *Evolution* 2001;**55**:2303–18.

Wilson VJ, Melvill Jones GM. *Mammalian Vestibular Physiology*. New York: Springer, 1979.

Yang A, Hullar TE. Relationship of semicircular canal size to vestibular-nerve afferent sensitivity in mammals. *Journal of Neurophysiology* 2007;**98**:3197–205.

Yi H. Using adaptive traits in the ear to estimate ecology of early snakes. In: Gower DJ, Zaher H (eds), *The Origin and Early Evolutionary History of Snakes*. Cambridge: Cambridge University Press, 2022, 271–93.

Yi H, Norell MA. The burrowing origin of modern snakes. *Science Advances* 2015;**1**:e1500743.

Zheng Y, Wiens JJ. Combining phylogenomic and supermatrix approaches, and a time-calibrated phylogeny for squamate reptiles (lizards and snakes) based on 52 genes and 4162 species. *Molecular Phylogenetics and Evolution* 2016;**94**:537–47.

Zug GR, Vitt LJ, Caldwell JP. *Herpetology: An Introductory Biology of Amphibians and Reptiles*, 2nd edn. London: Academic Press, 2001.